Report from the HERA Taskforce on Luminosity Optimization: Theory and First Luminosity Scans

M. Dohlus, G.H. Hoffstaetter[*], M. Lomperski, R. Wanzenberg

DESY, Notkestr. 85, 22603 Hamburg, Germany

January 29, 2003

[*]Now at Cornell University, Department of Physics, Laboratory of Elementary Particle Physics, Ithaca, NY 14850-5001, USA

1 Introduction

The phase space density of the colliding proton and positron beams and the focusing properties of the magnets determine the luminosity at the HERA experiments H1 and Zeus. The properties of the beams are described in terms of the beam emittance and the optical properties of the magnets in terms of the beta-function. In the following subsections the HERA parameters are introduced and it is explained how these parameters enter into several measurable quantities, like specific luminosity, beam spot size and tune shifts. Almost all measurable quantities depend on properties of the beam *and* the magnet lattice. Using several measurements it is the goal to disentangle the properties of the beam and properties of the magnet lattice.

1.1 Assumed parameters

The parameters of the upgraded HERA are discussed in Ref. [1]. For this paper we assume the parameters from table 1, which differ only with respect to the beam intensities from the parameters in [1] [1]. During the recommissioning phase of HERA we expect that the proton intensities will be not higher than the proton intensities in the year 2000 of about 90 mA to 100 mA in a typical luminosity run. Since the background situation at H1 and ZEUS is not yet good, after the installation of the upgraded interaction regions, we further assume that the positron intensity will not exceed 40 mA during the first luminosity running period.

1.2 Luminosity

For the reference parameter set (table 1) one obtains a Luminosity of

$$\mathcal{L}_0 = N_{cbun}\, f_0\, \frac{N_e\, N_p}{4\pi\, \sigma_{eff,x}\sigma_{eff,y}} = 3.59 \cdot 10^{31}\ \text{sec}^{-1}\ \text{cm}^{-2}, \tag{1}$$

where

$$\sigma_{eff,x} = \frac{1}{\sqrt{2}}\, \sqrt{\sigma_{ex}^2 + \sigma_{px}^2} = 112\,\mu\text{m}, \quad \sigma_{eff,y} = \frac{1}{\sqrt{2}}\, \sqrt{\sigma_{ey}^2 + \sigma_{py}^2} = 30\,\mu\text{m} \tag{2}$$

are the effective horizontal and vertical beam sizes.

The **specific Luminosity** is given by:

$$\mathcal{L}_{s0} = \frac{1}{e^2\, f_0}\, \frac{1}{4\pi\, \sigma_{eff,x}\, \sigma_{eff,y}} = 1.95 \cdot 10^{30}\ \text{sec}^{-1}\ \text{cm}^{-2}\ \text{mA}^{-2}, \tag{3}$$

---

[1]The electron and proton design currents are $I_e = 58$ mA and $I_p = 140$ mA (see ref. [1]).

		HERA		
Circumference	C_H	6335.83 m		
revolution frequency	f_0	47.317 kHz		
Number of colliding bunches	N_{cbun}	174		
		HERA-e		HERA-p
Energy	E_e	27.5 GeV	E_p	920 GeV
Total current	I_e	40 mA	I_p	90 mA
Number of bunches		189		180
Single bunch current	I_{be}	211 μA	I_{bp}	500 μA
Bunch Population	N_e	$2.79 \cdot 10^{10}$	N_p	$6.59 \cdot 10^{10}$
Emittance (one sigma)	ϵ_{ex}	20.0 nm	ϵ_{px}	5.1 nm
	ϵ_{ey}	3.4 nm	ϵ_{py}	5.1 nm
Invariant Emittance	ϵ_{Nex}	4.3 mm	ϵ_{Npx}	20 μm
$4\,\gamma\epsilon$ (two sigma)	ϵ_{Ney}	0.73 mm	ϵ_{Npy}	20 μm
Beta-functions at IP	β_{ex}	0.63 m	β_{px}	2.45 m
	β_{ey}	0.26 m	β_{py}	0.18 m
Beam size at IP	σ_{ex}	112.2 μm	σ_{px}	111.8 μm
	σ_{ey}	29.7 μm	σ_{py}	30.3 μm
Bunch length (rms)	σ_{ez}	10.3 mm	σ_{pz}	191 mm
$2.355\,\sigma_z/c$ (FWHM)	FWHM_{ez}	0.081 ns	FWHM_{pz}	1.5 ns

Table 1: Assumed HERA parameters. This parameter set is used in this report. Please note that though the design intensities differ from those in this list (see [1]), the beam dimensions at the interaction point are taken from the list of design parameters.

e is the charge of an electron. The specific Luminosity can be rewritten in terms of the beta-function at the interaction point and the beam emittance:

$$\mathcal{L}_s = \frac{1}{e^2\,f_0}\ \frac{1}{2\pi\,\sqrt{\beta_{ex}\,\epsilon_{ex} + \beta_{px}\,\epsilon_{px}}\,\sqrt{\beta_{ey}\,\epsilon_{ey} + \beta_{py}\,\epsilon_{py}}}. \qquad (4)$$

In equations (1) and (4) it has been assumed that the beam size does not vary over the bunch length. But the vertical beta-function of the proton beam is smaller than the design proton bunch length. Therefore the luminosity is smaller than calculated from Eqn.(1) and (4) due to the **hourglass effect**. The effective vertical and horizontal beam size at a distance s form the interaction point is

$$\sigma_{eff,x,y}(s) = \frac{1}{\sqrt{2}}\ \sqrt{\beta_{ex,y}\,\epsilon_{ex,y}\left(1 + \frac{s^2}{\beta_{ex,y}^2}\right) + \beta_{px,y}\,\epsilon_{px,y}\left(1 + \frac{s^2}{\beta_{px,y}^2}\right)}. \qquad (5)$$

A plot of the effective vertical and horizontal beam size (Eqn. (5)) is shown in Fig. 1. The specific luminosity is reduced by a factor of
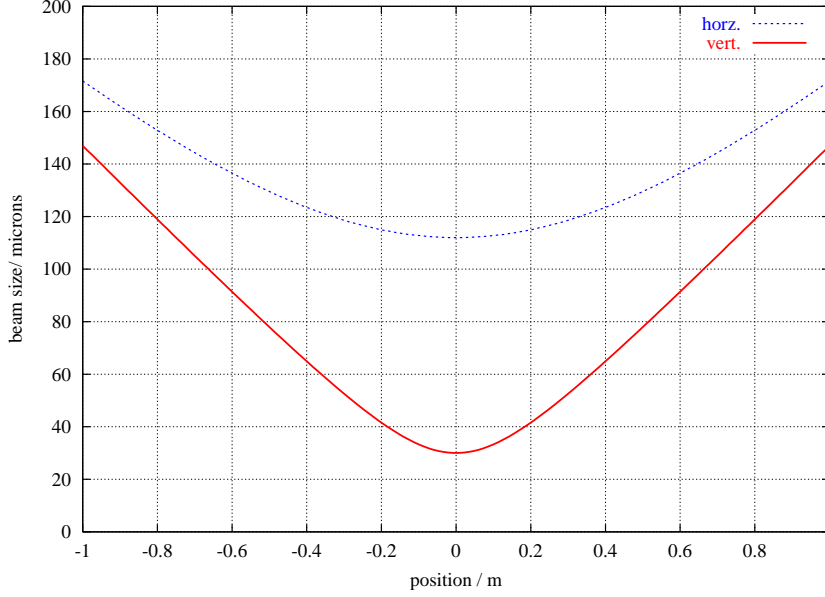
3

Figure 1: Effective beam size

$$\eta_A(\sigma_{ez}, \sigma_{pz}) = \frac{2}{\sqrt{\pi}} \sqrt{\frac{2}{\sigma_{ez}^2 + \sigma_{pz}^2}} \int_0^\infty ds \; \frac{\sigma_{eff,x}(0)\,\sigma_{eff,y}(0)}{\sigma_{eff,x}(s)\,\sigma_{eff,y}(s)} \; \exp\left(-s^2 \frac{2}{\sigma_{ez}^2 + \sigma_{pz}^2}\right)$$

(6)

due to the hourglass effect. The reduction factor $\eta_A(\sigma_{ez}, \sigma_{pz})$ as a function of the proton beam bunch length σ_{pz} is listed in the following table 2. The effect of the positron beam bunch length σ_{ez} can be neglected since $\sigma_{ez} \ll \sigma_{pz}$.

Bunch length		$\eta_A(\sigma_{ez}, \sigma_{pz})$	spez. Luminosity
FWHM / ns	σ_{pz} /mm		$\mathcal{L}_s$ / $\sec^{-1}\mathrm{cm}^{-2}\mathrm{mA}^{-2}$
0.0	0	1.0	$1.95 \cdot 10^{30}$
1.0	127	0.958	$1.87 \cdot 10^{30}$
1.5 (design)	191	0.919	$1.79 \cdot 10^{30}$
2.0	255	0.877	$1.71 \cdot 10^{30}$
2.5	318	0.835	$1.63 \cdot 10^{30}$
3.0	381	0.795	$1.55 \cdot 10^{30}$

Table 2: Reduction of the HERA luminosity due to the hourglass effect. The reduction factor and the resulting specific Luminosity has been calculated for different proton bunch lengths (the FWHM and rms values are listed).

To understand the deviation between calculated and measured values of the specific luminosity additional measurements of the beam emittance and further consistency checks are required.

The **photon spot size** (rms) at the Zeus and H1 luminosity monitor are

given by:

$$\sigma_{ph,x} = \sqrt{\frac{\epsilon_{ex}}{\beta_{ex}} d_{IP}{}^2 + \sigma_{res}^2 + \left(d_{IP}\frac{1}{\gamma_e}\right)^2} \quad = \quad 19.2\,\text{mm (Zeus)} \qquad (7)$$

$$= \quad 18.5\,\text{mm (H1)} \qquad (8)$$

$$\sigma_{ph,y} = \sqrt{\frac{\epsilon_{ey}}{\beta_{ey}} d_{IP}{}^2 + \sigma_{res}^2 + \left(d_{IP}\frac{1}{\gamma_e}\right)^2} \quad = \quad 12.5\,\text{mm (Zeus)} \qquad (9)$$

$$= \quad 12.0\,\text{mm (H1)}, \qquad (10)$$

where $d_{IP} = 107\,\text{m (Zeus)}; 103\,\text{m (H1)}$ is the distance between the interaction point and the luminosity monitor, $\sigma_{res} \approx 1.5\,\text{mm}$ is the resolution of the photon detector, $\gamma_e = 5.382 \cdot 10^4$ is the relativistic γ factor of the positron beam. The photon beam size can be used to determine the ratio between the emittance and the beta-function at the IP of the positron beam. For the assumed parameters one obtains:

$$\frac{\epsilon_{ex}}{\beta_{ex}} = 3.175 \cdot 10^{-8}, \qquad \frac{\epsilon_{ey}}{\beta_{ey}} = 1.308 \cdot 10^{-8}. \qquad (11)$$

1.3 Beam-Beam Tune shift

The proton beam acts as a quadrupole-like lens on the positron beam. The linear beam-beam parameter for the positrons is:

$$\xi_{ex} = \frac{1}{2\pi} \frac{N_p}{\sigma_{px}\,(\sigma_{px} + \sigma_{py})} \frac{r_e\,\beta_{ex}}{\gamma_e} = 2.18 \cdot 10^{-2} \qquad (12)$$

in the horizontal plane, and

$$\xi_{ey} = \frac{1}{2\pi} \frac{N_p}{\sigma_{py}\,(\sigma_{px} + \sigma_{py})} \frac{r_e\,\beta_{ey}}{\gamma_e} = 3.32 \cdot 10^{-2} \qquad (13)$$

in the vertical plane, where $r_e = 2.8179 \cdot 10^{-15}$ m is the classical radius of the electron and γ_e the relativistic γ-factor. The corresponding parameters for the proton beam are much smaller:

$$\xi_{px} = 1.069 \cdot 10^{-3}, \qquad \xi_{py} = 2.965 \cdot 10^{-4}. \qquad (14)$$

The parameter ξ_{ex} (ξ_{ey}) represents the horizontal (vertical) incoherent tune shift per IP of the positron beam. The coherent tune shift is approximately a factor two smaller than the incoherent one [2, 9]. For *two* IPs one expects approximately the following coherent tune shifts:

$$\Delta\nu_{ex} = \xi_{ex} \text{ or } f_0\,\Delta\nu_{ex} = 1.032\,\text{kHz} \qquad (15)$$

$$\Delta\nu_{ey} = \xi_{ey} \text{ or } f_0\,\Delta\nu_{ey} = 1.571\,\text{kHz}. \qquad (16)$$

The ratio between the vertical and horizontal tune shift does not depend on the beam intensities:

$$\frac{\Delta\nu_{ey}}{\Delta\nu_{ex}} = \frac{\beta_{ey}}{\beta_{ex}}\frac{\sigma_{px}}{\sigma_{py}} = 1.523 \,. \tag{17}$$

This equation may be rewritten in the following form:

$$\frac{\Delta\nu_{ey}}{\Delta\nu_{ex}}\sqrt{\frac{\epsilon_{Npy}}{\epsilon_{Npx}}} = \frac{\beta_{ey}}{\beta_{ex}}\sqrt{\frac{\beta_{px}}{\beta_{py}}}\,. \tag{18}$$

Once the emittance of the proton beam is measured (e.g. using a wire scanner) the ratio of vertical to horizontal beam-beam tune shift presents the ratio of the beta-functions at the interaction point according to Eqn. (18).

2 Luminosity optic

In the year 2002 the optic "helumgj" (provided by E. Gianfelice) is used in the HERA positron ring, while the optic "hpl920e+" (provided by B. Holzer) is used in the HERA proton ring. The interaction region East is used as the starting point for optics calculations with the HERA database. The beta-functions at the interaction regions are summarized in Table 3. Both beams collide in the interaction region South (ZEUS) and North (H1). An overview of the magnet lattice of these interaction regions is shown in Fig. 2.

region	s / m	HERA-e β_x/m	β_y/m	HERA-p β_x/m	β_y/m
East	0.00	2.95	1.94	19.98	2.00
South	1583.96	0.62	0.26	2.45	0.18
West	3167.91	14.61	32.11	37.31	37.35
North	4751.86	0.62	0.26	2.45	0.18
East	6335.82				

Table 3: Beta-functions in the luminosity optic for the HERA rings.
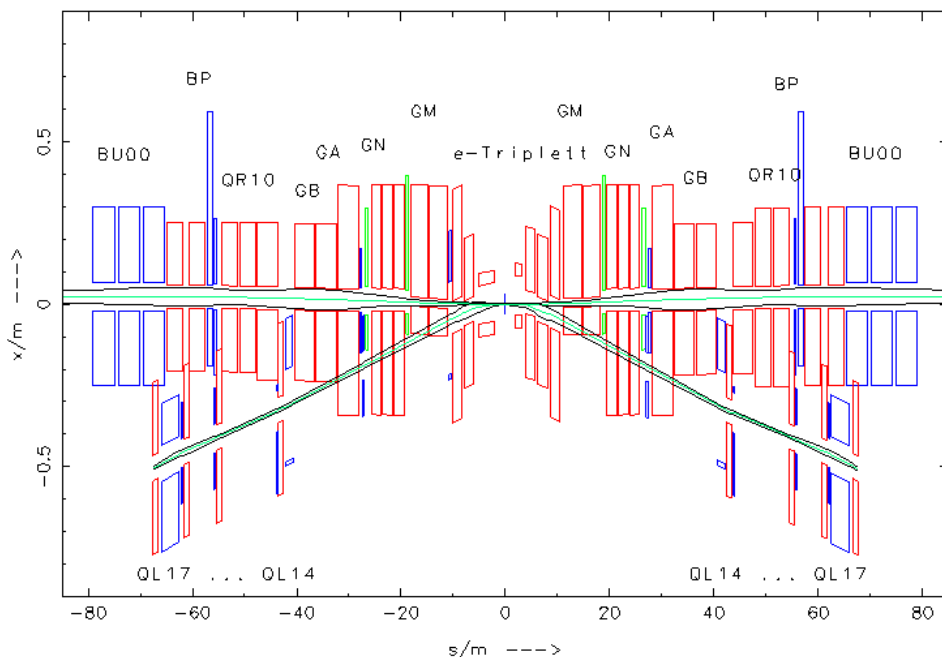
Figure 2: Magnet configuration of the (upgraded) HERA interaction regions in the South and North [3]

A plot of beta-functions and the magnet lattice in the interaction region South of the HERA-p and HERA-e rings is shown Fig. 3 and Fig. 4. A more detailed plot of the beta-functions near the interaction region South is given in Figs. 5, 6 and 7. The position of the interaction point South has been set to zero in these
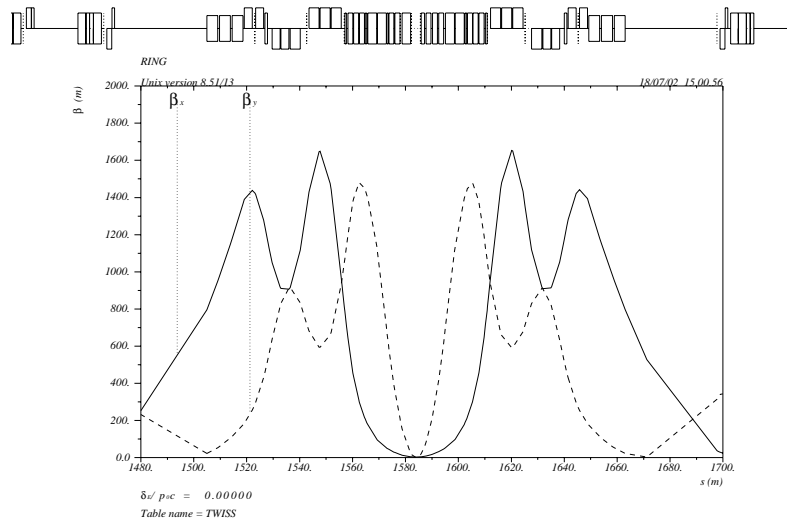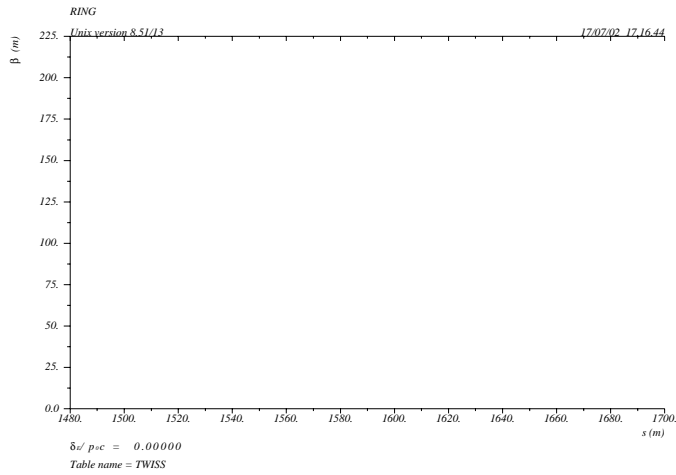
Figure 3: Luminosity optic of interaction region South of the HERA-p ring.

three plots. In the HERA-p ring the beta-functions are symmetric with respect to the interaction point (see Fig. 5), while in the HERA-e ring an asymmetric lattice configuration has been chosen as shown in Fig. 6.
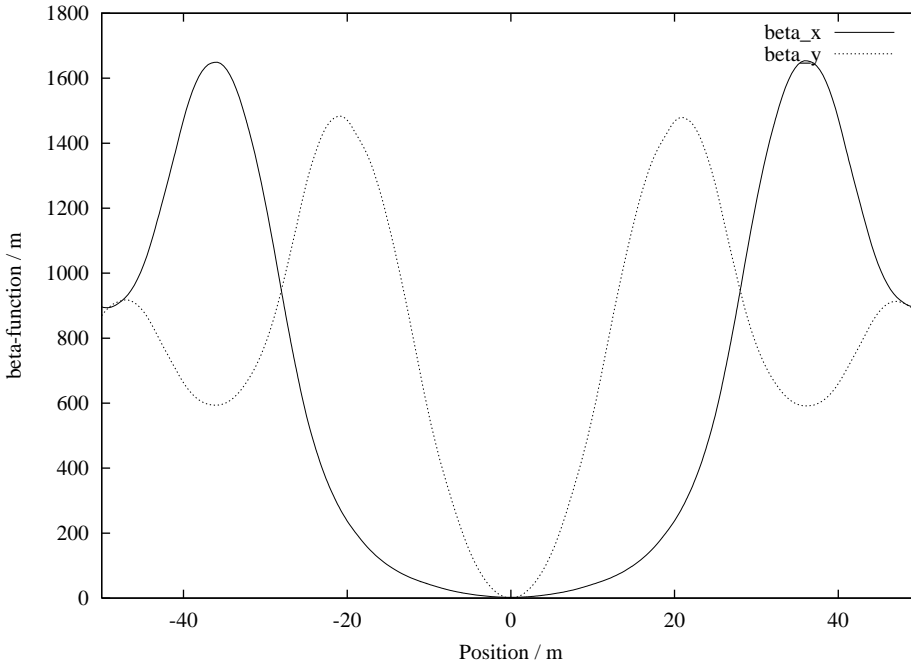

Figure 5: Horizontal and vertical beta-functions near the interaction point South of the HERA-p ring.

2.1 Luminosity bumps

Closed orbit bumps are used to adjust the position of the positron and the proton beam at the interaction point. Four corrector magnets are used in each bump. The ratios of the kicks and the names of the corrector magnets are listed in tables 4 and 5 for the interaction point South. The bumps for the interaction point North differ only with respect to the names of the corrector magnets. In Fig. 8 and Fig. 9 plots are shown of the horizontal and vertical for an orbit deviation in the closed bump of 1 mm at the interaction point. The corresponding kick of the first corrector is given in tables 4 and 5. The kicks of the other correctors are completely determined by the condition that this bump creates no slope at the interaction point and that the bump is closed. The kick ratio (normalized to the first corrector) are also included in tables 4 and 5. The bumps in the HERA p-ring (Fig. 9) used for the luminosity scans are described in the next section.
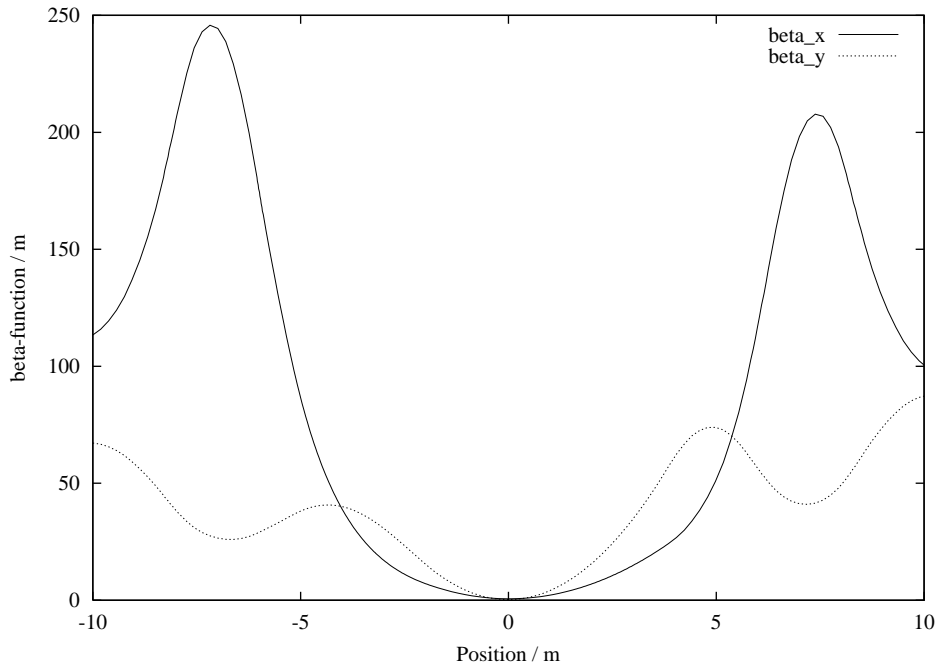
Figure 6: Horizontal and vertical beta-functions near the interaction point South of the HERA-e ring.
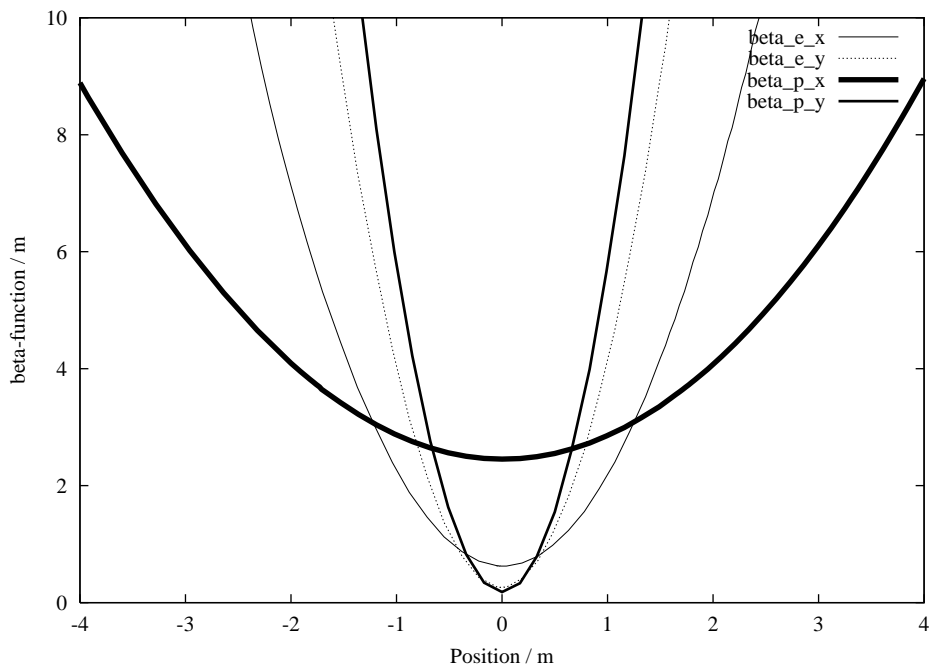

Figure 7: Detailed view of the horizontal and vertical beta-functions near the interaction point South of the HERA-e and HERA-p ring.
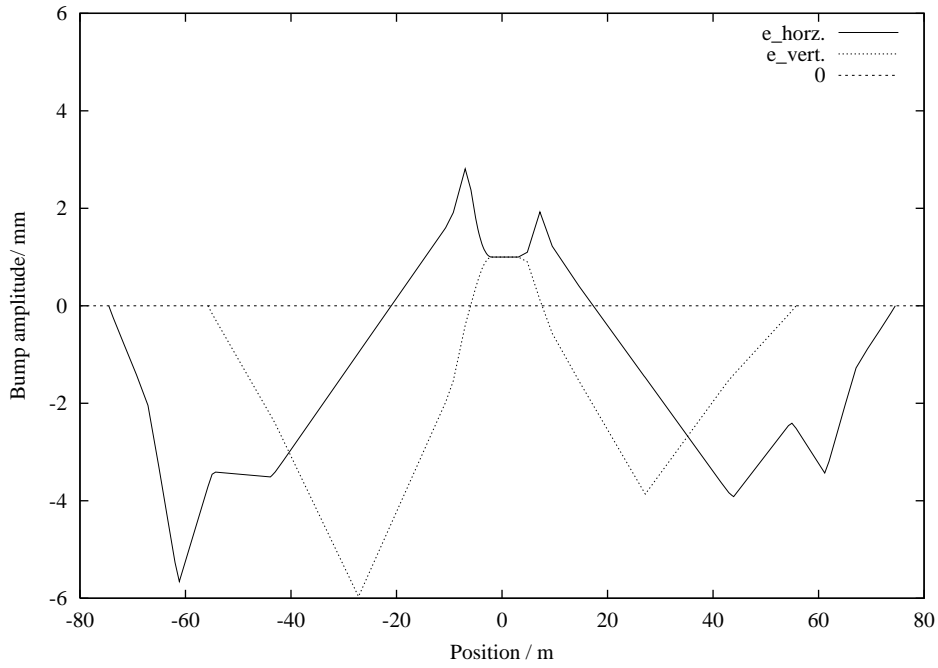
10

Figure 8: Horizontal and vertical bumps (4 correctors) used to change the positron of the beam at an interaction point in the HERA-e ring.
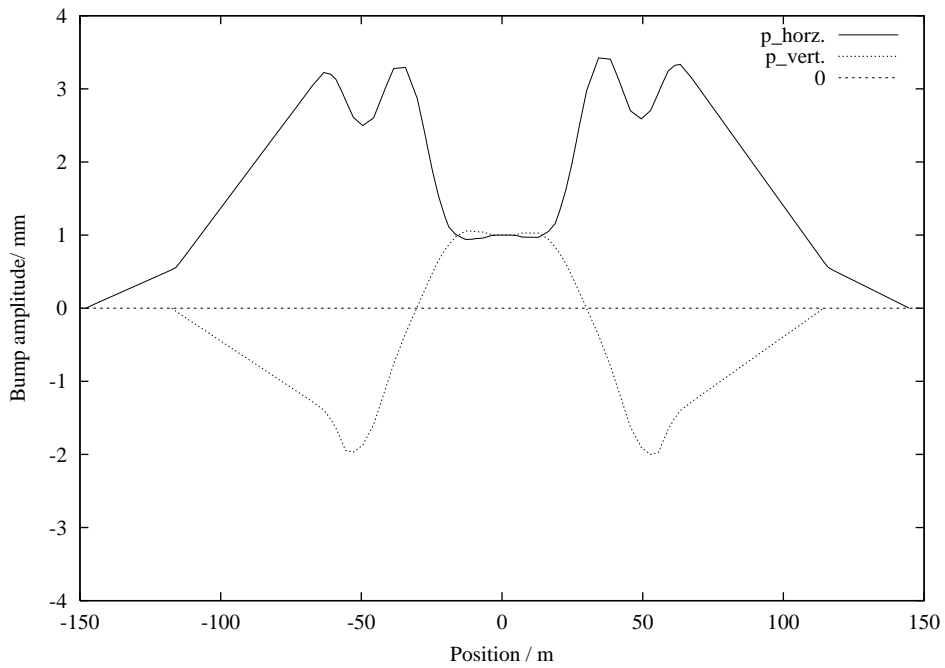

Figure 9: Horizontal and vertical bumps (4 correctors) to change the position of the proton beam at an interaction point in the HERA-p ring.

11

corrector	kick ratio	$\beta_x/$m	$\phi_x/2\,\pi$	kick, offset
SL 75 CH	1.0000	13.21	12.793	-0.292 mrad
SL 44 CH	-0.3848	12.18	13.095	
IP		0.63	13.487	1 mm
SR 44 CH	-0.7369	19.60	13.871	
SR 75 CH	0.6218	23.83	14.107	
corrector	kick ratio	$\beta_y/$m	$\phi_y/2\,\pi$	kick, offset
SL 56 CV	1.0000	49.42	12.284	-0.206 mrad
SL 27 CV	-2.2622	33.48	12.409	
IP		0.26	12.707	1 mm
SR 27 CV	-1.6131	22.49	13.065	
SR 56 CV	0.6407	40.74	13.356	

Table 4: Corrector magnets and kick ratios of the bumps of the HERA-e ring used to change the position of the beam at the interaction point South.

corrector	kick ratio	$\beta_x/$m	$\phi_x/2\,\pi$	kick, offset
SL148 CX	1.0000	56.22	7.241	0.0194 mrad
BQ01 SL	2.7714	198.19	7.650	
IP		2.45	7.880	1 mm
BQ01 SR	2.7272	198.72	8.110	
SR145 CX	0.9894	52.16	8.509	
corrector	kick ratio	$\beta_y/$m	$\phi_y/2\,\pi$	kick, offset
SL117 CY	1.0000	333.66	7.579	-0.02799 mrad
SL 56 BZ	-2.8254	547.83	8.053	
IP		0.18	7.880	1 mm
SR 56 BZ	-2.8621	544.82	8.564	
SR114 CY	0.9740	326.78	9.037	

Table 5: Corrector magnets and kick ratio of the bumps of the HERA-p ring used to change the position of the beam at the interaction point South.

2.2 Dynamic beta-functions

The nominal beta-functions at the interaction point (see table 1) correspond to a zero beam current situation, i.e. the beam-beam force is zero. The actual (dynamic) beta-functions depend on the strength of the beam-beam force. The effect of the beam-beam force due to the proton beam on the positron beam is the dominant beam-beam effect. The quadrupole strength k of the beam-beam lens may be written in terms of the beam-beam parameter $\xi_{ex,y}$ (Eqn. 12 and 13):

$$k_x = \frac{1}{l}\frac{4\,\pi}{\beta_{ex}}\,\xi_{ex}, \quad k_y = \frac{1}{l}\frac{4\,\pi}{\beta_{ey}}\,\xi_{ey}, \tag{19}$$

l is the effective length of the beam-beam lens and β_{ex} and β_{ey} are the nominal horizontal and vertical beta-functions at the interaction point. The beam-beam quadrupole strength in terms of the total proton current I_p (180 bunches) is:

$$k_x = 4.8328 \cdot 10^{-2} \mathrm{m}^{-2} \frac{I_p}{\mathrm{mA}}, \quad k_y = 17.8298 \cdot 10^{-2} \mathrm{m}^{-2} \frac{I_p}{\mathrm{mA}}. \qquad (20)$$

The beam-beam quadrupole is defocusing in both planes. The computer code MAD [5] has been used to calculate the effect of the beam-beam lens on the beta-functions of the HERA-e ring after the tune has been rematched to the values without the beam-beam lens. Two cases have been considered:

a) betatron-tunes close to the integer resonances $Q_x = 54.102$ and $Q_y = 51.213$ (usually used during lumi-runs before the luminosity upgrade) and

b) betatron-tunes $Q_x = 54.239$ and $Q_y = 51.315$ which are usually used during positron injection and during the ramp. To obtain a high polarization it is important to use tunes close to the integer resonance.

The results for the dynamic (beam-beam force) beta-function in the HERA-e ring are shown in Fig. 10 as a function of the total proton current. For a total proton current of 90 mA the results are further summarized in table 6. The specific luminosities have been calculated with and without the hourglass effect. The beam-beam force will increase the beta-function and therefore decrease the the specific luminosity by a factor of 0.9 for the tunes $Q_x = 54.102$ and $Q_y = 51.213$. The hourglass effect is slightly mitigated due to the larger (dynamic) beta-functions. During the luminosity runs in 2002 the tunes $Q_x = 54.239$ and $Q_y = 51.315$ have been used. For these tunes we expect an specific luminosity of $1.73 \cdot 10^{30} \sec^{-1} \mathrm{cm}^{-2} \mathrm{mA}^{-2}$ with a total proton current of 90 mA.

I_p /mA	0	90	90
Q_{ex}		54.102	54.239
Q_{ey}		51.213	51.315
β_{ex} /m	0.62	0.77	0.64
β_{ey} /m	0.26	0.33	0.30
$\mathcal{L}_{s0}$ / $10^{30} \sec^{-1} \mathrm{cm}^{-2} \mathrm{mA}^{-2}$	1.95	1.74	1.88
$\eta_A(\sigma_{ez}, \sigma_{pz})$	0.919	0.931	0.925
$\mathcal{L}_s$ / $10^{30} \sec^{-1} \mathrm{cm}^{-2} \mathrm{mA}^{-2}$	1.79	1.62	1.73

Table 6: Dynamic beta-functions in the luminosity optic for the HERA-e ring. The specific luminosity is calculated without ($\mathcal{L}_{s0}$) and with ($\mathcal{L}_s$) the hourglass effect for a proton bunch length of 1.5 ns (FWHM).
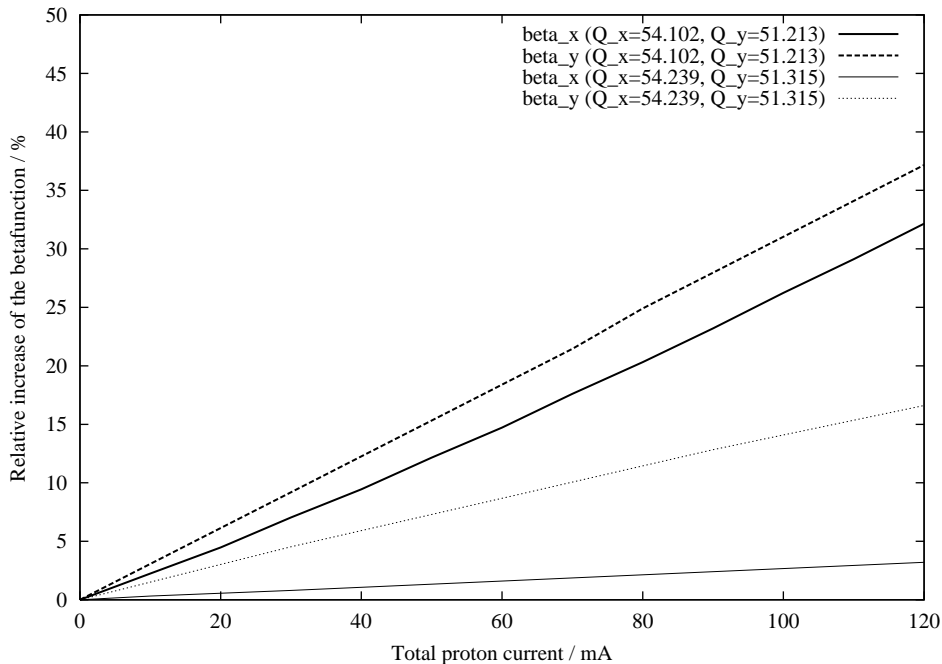
Figure 10: Horizontal and vertical dynamic beta-function at the interaction point as a function of the total (180 bunches) proton current for two sets of betatron tunes.

2.3 Influence of the rf frequency shift on the beta-function

The beam emittance is determined from so-called radiation damping and quantum excitation. The equilibrium emittance can be calculated as [6]:

$$\epsilon_{ex} = \frac{C_q \gamma^2}{J_x} \left(\frac{\int ds \, \mathcal{H}/\rho^3}{\int ds \, 1/\rho^2} \right), \tag{21}$$

here $C_q = 3.84 \, 10^{-13}$ m is a constant, γ the relativistic gamma factor of the beam, ρ the local bending radius of the magnetic guide field, J_x the horizontal damping partition number, and $\mathcal{H}(s)$ is defined in [6] (Eqn. (5.71)). To decrease the emittance of the HERA positron beam the rf frequency is increased by about 300 Hz. This rf frequency shift decreases the average radius of the orbit and changes the damping partition number and the synchrotron radiation integrals which define the horizontal emittance according to equation (21).

The effect of the rf frequency shift can be simulated with the optic codes PETROS [7] or MAD [5] using an equivalent momentum deviation of

$$\frac{\Delta p}{p} = -\alpha_p \frac{\Delta f_{rf}}{f_{rf}}, \tag{22}$$

where $\alpha_p = 4.751 \, 10^{-4}$ is the momentum compaction factor of the luminosity optic. The luminosity optic "helumgj" has been matched for $\Delta p/p = 0$. The

beta-functions from table 3 correspond to the case $\Delta p/p = 0$, i.e. no rf frequency shift. Simulations with PETROS and MAD show that if not compensated there is a tune dependent influence of the rf frequency shift on the beta-functions in the interaction regions. The results are summarized in table 7. The first column shows the reference values which are valid for $\Delta p/p = 0$ and both considered sets of betatron tunes. The effect of the rf frequency shift on the beta-functions is small for the tunes $Q_{ex} = 54.239$ and $Q_{ey} = 54.239$, while an increase of up-to 13 % of the horizontal beta-function is found for the tunes $Q_{ex} = 54.102$ and $Q_{ey} = 54.213$.

$\Delta p/p$	0	-0.00133	-0.00133
Q_{ex}		54.102	54.239
Q_{ey}		51.213	51.315
β_{ex} /m South	0.62	0.70	0.63
β_{ey} /m	0.26	0.28	0.28
β_{ex} /m North	0.62	0.68	0.62
β_{ey} /m	0.26	0.26	0.26

Table 7: Influence of the rf frequency shift on the beta functions in the South and North interaction regions.

3 Luminosity scans for beam size determination

At HERA beam separation scans have been used several times, starting in 1994 [8], to determine the specific luminosity. Three different methods [10] of cross calibrating beam profile measurements and luminosity measurements will here be derived. The recent experimental results are reported in sections 5 and 6.

3.1 Different methods

The specific luminosity $\mathcal{L}_s$ for head-on collisions of two beams with densities ρ_p and ρ_e is given by

$$\mathcal{L}_s = \frac{1}{f_0\, q_p\, q_e} \int_\infty [\int_{-\infty}^\infty \rho_p(x,y,z)dz]\, [\int_{-\infty}^\infty \rho_e(x,y,z)dz]\, dxdy \ , \qquad (23)$$

where the circulation frequency f_0 and the charges q_p and q_e of the particles in the two beams have been used. During a luminosity scan, the distance between the center of the two beams is varied. We let the densities ρ_p and ρ_e describe a centered beam, i.e. $\int_\infty \vec{r}\rho_i(x,y,z)d\vec{r} = 0$. Then the luminosity scan in the x–direction is described by

$$\mathcal{L}_s^x(\Delta x) = \frac{1}{f_0\, q_p\, q_e} \int_\infty [\int_{-\infty}^\infty \rho_p(x,y,z)dz]\, [\int_{-\infty}^\infty \rho_e(x-\Delta x,y,z)dz]dxdy \ . \qquad (24)$$

When $\bar{\rho}(y) = \int_\infty \rho(x,y,z)dxdz$ is the projected density, the luminosity scan in the x-direction gives information about the vertical density:

$$\int_{-\infty}^\infty \mathcal{L}_s^x(\Delta x)d\Delta x = \frac{1}{fq_pq_e} \int_\infty \bar{\rho}_p(y)\bar{\rho}_e(y)dy \ . \qquad (25)$$

Assuming Gaussian beams for protons: $\rho_p(x,y,z) = G^{\sigma_{xp}}(x)G^{\sigma_{yp}}(y)\rho_{zp}(z)$, and equally for electrons, with the following convolution property:

$$G^\sigma(x) = \frac{1}{\sqrt{2\pi}\sigma} \exp(-\frac{x^2}{2\sigma^2}) \ , \quad \int_\infty G^{\sigma_1}(x-\tilde{x})G^{\sigma_2}(x)dx = G^{\sqrt{\sigma_1^2+\sigma_2^2}}(\tilde{x}) \ , \qquad (26)$$

the integral in equation (25) evaluates with $\bar{\rho}_p(y) = G^{\sigma_{yp}}(y)$, $\bar{\rho}_e(y) = G^{\sigma_{ye}}(y)$ to

$$\int_{-\infty}^\infty \mathcal{L}_s^x(\Delta x)d\Delta x = \frac{1}{fq_pq_e} \frac{1}{\sqrt{2\pi}(\sigma_{yp}^2+\sigma_{ye}^2)} \ . \qquad (27)$$

A related property which also required integrals over luminosity scans was used at the CERN ISR for luminosity calibration [12, 13].

For product densities $\rho(x,y,z) = \rho_x(x)\rho_y(y)\rho_z(z)$, the second moments $< x^2 >_e$ and $< y^2 >_e$ of the positron beam can be obtained by a luminosity scan, when

16

the second order moments of the proton beam are known since the second order moment of the luminosity scan is given by

$$
\begin{aligned}
< x^2 >_{\mathcal{L}_s^x} &= \frac{\int_{-\infty}^{\infty} \mathcal{L}_s^x(\Delta x)\Delta x^2 d\Delta x}{\int_{-\infty}^{\infty} \mathcal{L}_s^x(\Delta x)d\Delta x} \\
&= \frac{\int_{-\infty}^{\infty}\int_{\infty} \rho_{xp}(x)\rho_{yp}(y)\rho_{xe}(x-\Delta x)\rho_{ye}(y)dxdy\Delta x^2 d\Delta x}{\int_{-\infty}^{\infty} \rho_{yp}(y)\rho_{ye}(y)dy} \\
&= \int_{-\infty}^{\infty}\int_{\infty} \rho_{xp}(x)\rho_{xe}(\tilde{x})(x-\tilde{x})^2 dxd\tilde{x} = < x^2 >_p + < x^2 >_e \ .
\end{aligned}
\tag{28}
$$

Here it has been used that the first moment $< x >$ of a centered beam vanishes. It is important to note that this relation of the second order moments holds for all product densities and no specific knowledge on ρ_p is required to determine $< x^2 >_e$. With these properties we can use the following three methods to determine the overlap beam sizes $\Sigma_x = \sqrt{< x^2 >_p + < x^2 >_e}$ and $\Sigma_y = \sqrt{< y^2 >_p + < y^2 >_e}$.

Method (a): The standard deviation $< x^2 >_{\mathcal{L}_s^x}$ of the luminosity scan is obtained by fitting a_x, b_x, and c_x of a bell curve $a_x \exp(-b_x(x-c_x)^2)$ to the data. Then one obtains $\Sigma_x = 1/\sqrt{2b_x}$. Similarly one obtains $\Sigma_y = 1/\sqrt{2b_y}$. Assuming Gaussian beams with the convolution property stated in Eqn. (26) the luminosity scan data should be approximated by

$$
\mathcal{L}_s^x(\Delta x, \Delta_y) = \frac{1}{f_0 q_p q_e} \frac{1}{2\pi \Sigma_x \Sigma_y} e^{-\frac{\Delta_x}{2\Sigma_x^2}} e^{-\frac{\Delta_y}{2\Sigma_y^2}} \ .
\tag{29}
$$

Method (b): It is assumed that both beams have a Gaussian density, which leads to

$$
f_0 q_p q_e \int_{\infty} \mathcal{L}_s^x(\Delta x)d\Delta x = \int_{-\infty}^{\infty} \frac{e^{-\frac{y^2}{2\sigma_{py}^2}}}{\sqrt{2\pi}\sigma_{py}} \frac{e^{-\frac{y^2}{2\sigma_{ey}^2}}}{\sqrt{2\pi}\sigma_{ey}} dy = \frac{1}{\sqrt{2\pi}\sqrt{\sigma_{py}^2 + \sigma_{ey}^2}} \ .
\tag{30}
$$

In this method, the vertical overlap beam size is obtained from the horizontal luminosity scan with $\Sigma_y = (\sqrt{2\pi}f q_p q_e \int_{\infty} \mathcal{L}_s^x(\Delta x)d\Delta x)^{-1}$ and vice versa. The integral is evaluated by fitting a_x, b_x, and c_x of a bell curve $a_x \exp(-b_x(x-c_x)^2)$ to the data. Then one obtains $\Sigma_y = \sqrt{b_x}(\sqrt{2\pi}f q_p q_e a_x)^{-1}$ and similarly $\Sigma_y = \sqrt{b_x}(\sqrt{2\pi}f q_p q_e a_x)^{-1}$. Also for these Σ_x and Σ_y, the luminosity scan data should be approximated by equation (29).

Method (c): Only assuming product distributions for the two beams, equation (28) is used to find

$$
\Sigma_x = \frac{\int_{-\infty}^{\infty} \mathcal{L}_s^x(\Delta x)\Delta x^2 d\Delta x}{\int_{-\infty}^{\infty} \mathcal{L}_s^x(\Delta x)d\Delta x} \quad , \quad \Sigma_y = \frac{\int_{-\infty}^{\infty} \mathcal{L}_s^y(\Delta y)\Delta y^2 d\Delta y}{\int_{-\infty}^{\infty} \mathcal{L}_s^y(\Delta y)d\Delta y} \ .
\tag{31}
$$

17

To check how well the data of the luminosity scan can be approximated by a Gaussian, two checks can be performed. (1) One can compare the data with the curve of equation (29). This Gaussian Luminosity scan curve has the Σ_x and Σ_y of equation (31). However, it might not have the integral $\int_{-\infty}^{\infty} \mathcal{L}_s^x(\Delta x) d\Delta x$ which one obtains from the data. (2) One can alternatively assume Gaussian beam distributions and compute $\Sigma_y = (\sqrt{2\pi} f q_p q_e \int_{\infty} \mathcal{L}_s^x(\Delta x) d\Delta x)^{-1}$ and similarly Σ_x by integrating the luminosity scan data. Subsequently one can compare the resulting curve of equation (29) with the data points.

The range of applicability of the first two methods (a) and (b) is restricted since it is required that the luminosity scan data can be fitted well by a bell curve, and in case of (b) each beam distribution has to be approximately Gaussian. Method (c) does not have this restriction. On the other hand, these two methods have the advantage that they can be evaluated even when the data points of the luminosity scan are too sparse to allow for an accurate evaluation of the integrals in equation (31). The most accurate method (c) requires many data points which go up to large scan amplitudes Δx and Δy.

3.2   Influence of the beam-beam force

Here we will consider two effects of the beam–beam force on the luminosity scan. Firstly the beam–beam kick leads to a displacement of the e^+ beam from the proton beam which adds to the displacement which is produced by the symmetric bump during the scan. Secondly the strength of the beam–beam lens changes during the luminosity scan. This leads to a changing beta-function and therefore a changing e^+ beam size during the luminosity scan. The beam–beam potential for a Gaussian proton beam with beam sizes σ_{xp} and σ_{yp} at the interaction point is given by [14]

$$U(x,y) = \int_0^\infty \frac{e^{-\frac{x^2}{2(\sigma_{px}^2+t)} - \frac{y^2}{2(\sigma_{py}^2+t)}}}{\sqrt{\sigma_{px}^2+t}\sqrt{\sigma_{py}^2+t}} dt \ . \tag{32}$$

The kick on an e^+ passing the proton beam in the distance (x,y) from its center is given by

$$\delta \vec{r}' = -C_{bb} \ \partial_{\vec{r}} U(x,y) \ \text{with} \ C_{bb} = \frac{q_p}{q_e} \frac{N_p \, r_e}{\gamma_e}, \tag{33}$$

$r_e = 2.8$ fm being the classical electron radius and γ_e being the positrons relativistic factor. The number of protons in the colliding bunch is given by N_p.

When the one turn transport matrix without the beam–beam interaction is denoted by $\underline{M}_0$ and the beam–beam kick $\Delta x'$ is given, the position and slope deviation at the interaction point satisfy

$$\underline{M} \begin{pmatrix} \delta x \\ \delta x' \end{pmatrix} + \begin{pmatrix} 0 \\ \Delta x' \end{pmatrix} = \begin{pmatrix} \delta x \\ \delta x' \end{pmatrix} \ , \quad \begin{pmatrix} \delta x \\ \delta x' \end{pmatrix} = (\underline{1} - \underline{M})^{-1} \begin{pmatrix} 0 \\ \Delta x' \end{pmatrix} \ . \tag{34}$$

18

With the tunes Q_x^e, Q_y^e and the beta-functions β_x^e, β_y^e at the interaction point of the electron ring without beam–beam force, this leads to $\delta x = \frac{\beta_x^e}{2\tan(\pi Q_x^e)}\Delta x'$. When the symmetric bump separates the beams by the amount Δx_0, the actual distance Δx between the beams is given by the implicit solution of

$$\Delta x = \Delta x_0 + \delta x = \Delta x_0 - \frac{\beta_x^e}{2\tan(\pi Q_x^e)}C_{bb}\partial_{\bar{r}}U(\Delta x,0) \ . \tag{35}$$

The luminosity scan therefore should not be interpreted as a function of δ but as a function of the implicit solution Δx in order to eliminate the effect of the beam–beam kick.

Additionally one can take into account of the beam–beam lens and its disturbance of the beta-function. This leads to a focusing error at the interaction point which is characterized by $\delta k_x = -C_{bb}\partial_x^2 U(x,y)$ and $\delta k_y = -C_{bb}\partial_y^2 U(x,y)$. In the x–direction, the one turn matrix with beam–beam lens is given by

$$\underline{M} = \begin{pmatrix} 1 & 0 \\ -\frac{\delta k_x}{2} & 1 \end{pmatrix} \underline{M}_0 \begin{pmatrix} 1 & 0 \\ -\frac{\delta k_x}{2} & 1 \end{pmatrix} \ . \tag{36}$$

This leads to $\mathrm{tr}(M) = \mathrm{tr}(M_0) - \delta k_x M_{012} = 2\cos(2\pi Q_x^e) - \delta k_x \beta_x^e \sin(2\pi Q_x^e)$ and $M_{12} = M_{012} = \beta_x^e \sin(2\pi Q_x^e)$. The beta-function with the beam–beam lens is then given by $\beta_{bbx}^e = M_{12}/\sqrt{1 - [\frac{1}{2}\mathrm{tr}(M)]^2}$ leading to

$$\begin{aligned}
\delta\beta_x^e(x,y) &= \frac{\beta_{bbx}^e - \beta_x^e}{\beta_x^e} = \frac{\sin(2\pi Q_x^e)}{\sqrt{1 - [\cos(2\pi Q_x^e) - \frac{\delta k_x}{2}\beta_x^e \sin(2\pi Q_x^e)]^2}} - 1 \\
&= \frac{1}{\sqrt{1 - (\frac{\delta k_x \beta_x^e}{2})^2 + \frac{\delta k_x \beta_x^e}{\tan(2\pi Q_x^e)}}} - 1 \ . \tag{37}
\end{aligned}$$

After the overlap beam sizes Σ_x and Σ_y have been determined by applying method (a) to the luminosity scan data which has been corrected for the beam–beam kick, one can then use the proton emittances obtained from the wire scanner to compute the e^+ emittances by

$$\epsilon_x^e = \frac{\Sigma_x^2 - \beta_x^p \epsilon_x^p}{\beta_x^e[1 + \delta\beta_x^e(0,0)]} \tag{38}$$

and by the corresponding equation for the y–direction. For two Gaussian beams with overlap beam sizes Σ_x and Σ_y which do not change during the luminosity scan, equation (29) leads to

$$\mathcal{L}_s^x(\Delta x) = \frac{1}{f_0\,q_p\,q_e}\frac{1}{2\pi\Sigma_x\Sigma_y}e^{-\frac{\Delta x^2}{2\Sigma_x^2}} \ . \tag{39}$$

19

Assuming the e^+ emittances from equation (38) to be invariant during the luminosity scan, but taking the varying beam–beam lens into account therefore leads to

$$
\mathcal{L}_s^x(\Delta x) \;=\; \frac{1}{f q_p q_e} \frac{1}{\Sigma_x(\Delta x)\Sigma_y(\Delta x)} \exp\left(-\frac{\Delta x^2}{2\Sigma_x(\Delta x)^2}\right) , \tag{40}
$$

$$
\Sigma_x(\Delta x) \;=\; \sqrt{\epsilon_x^p \beta_x^p + \epsilon_x^e \beta_x^e [1 + \delta\beta_x^e(\Delta x, 0)]} , \tag{41}
$$

$$
\Sigma_y(\Delta x) \;=\; \sqrt{\epsilon_y^p \beta_y^p + \epsilon_y^e \beta_y^e [1 + \delta\beta_y^e(\Delta x, 0)]} . \tag{42}
$$

This difference between the plain Gaussian luminosity scan curve and equation (42) is not taken into account when fitting a Gaussian to luminosity scan data. To correct for the difference between equation (39) and (42), this difference is subtracted from the specific luminosity data. The obtained data points which are now corrected for the beam–beam kick and for the beam–beam lens should be described better by a Gaussian than the original data. Finally the standard deviation of the Gaussian fitted to these manipulated data points is used to compute the overlap beam sizes by the methods (a).

The beam–beam forces and the strength of the beam–beam lens will now be computed. With $\Delta = \sigma_x^2 - \sigma_y^2$ and $\sigma_x > \sigma_y$ one obtains the following derivatives of the beam–beam potential in equation (32) which will be used to determine the beam–beam kicks and the varying beta-functions:

$$
\partial_x U|_{y=0} \;=\; -x \int_0^\infty \frac{e^{-\frac{x^2}{2(\sigma_{xp}^2+t)}}}{\sqrt{\sigma_{xp}^2+t}^3 \sqrt{\sigma_{yp}^2+t}} dt \;.=\; -x \int_0^{\frac{1}{\sigma_x^2}} \frac{e^{-\frac{x^2}{2}t}}{\sqrt{1-t\Delta}} dt \tag{43}
$$

$$
\;=\; -\frac{x}{\Delta} e^{-\frac{x^2}{2\Delta}} \int_{\frac{\sigma_y^2}{\sigma_x^2}}^1 \frac{e^{\frac{x^2}{2\Delta}t}}{\sqrt{t}} dt \;=\; -2\sqrt{\frac{2}{\Delta}} e^{-\frac{x^2}{2\Delta}} \int_{\frac{x}{\sqrt{2\Delta}}\frac{\sigma_y}{\sigma_x}}^{\frac{x}{\sqrt{2\Delta}}} e^{t^2} dt \;. \tag{44}
$$

With the error function $\mathrm{erf}(x) = \frac{2}{\sqrt{\pi}} \int_0^x \exp(-x^2) dx$ and with $\mathrm{erfi}(x) = \frac{2}{\sqrt{\pi}} \int_0^x \exp(x^2) dx$ this leads to

$$
\partial_x U|_{y=0} \;=\; -\sqrt{\frac{2\pi}{\Delta}} e^{-\frac{x^2}{2\Delta}} \left[\mathrm{erfi}\left(\frac{x}{\sqrt{2\Delta}}\right) - \mathrm{erfi}\left(\frac{x}{\sqrt{2\Delta}}\frac{\sigma_y}{\sigma_x}\right)\right] ,
$$

$$
\partial_x^2 U|_{y=0} \;=\; \sqrt{\frac{2\pi}{\Delta}}\frac{x}{\Delta} e^{-\frac{x^2}{2\Delta}} \left[\mathrm{erfi}\left(\frac{x}{\sqrt{2\Delta}}\right) - \mathrm{erfi}\left(\frac{x}{\sqrt{2\Delta}}\frac{\sigma_y}{\sigma_x}\right)\right] - \frac{2}{\Delta}\left[1 - e^{-\frac{x^2}{2\sigma_x^2}}\frac{\sigma_y}{\sigma_x}\right] , \tag{45}
$$

$$
\partial_y U|_{y=0} \;=\; 0 , \tag{46}
$$

$$
\partial_y^2 U|_{y=0} \;=\; -\int_0^{\frac{1}{\sigma_x^2}} \frac{e^{-\frac{x^2}{2}t}}{\sqrt{1-t\Delta}^3} dt \;=\; -\frac{x}{\sqrt{2\Delta}}\frac{2}{\Delta} e^{-\frac{x^2}{2\Delta}} \int_{\frac{x}{\sqrt{2\Delta}}\frac{\sigma_y}{\sigma_x}}^{\frac{x}{\sqrt{2\Delta}}} \frac{e^{t^2}}{t^2} dt \tag{47}
$$

$$
\;=\; -\frac{x}{\sqrt{2\Delta}}\frac{2}{\Delta} e^{-\frac{x^2}{2\Delta}} \left\{[-\frac{e^t}{t} dt]_{\frac{x}{\sqrt{2\Delta}}\frac{\sigma_y}{\sigma_x}}^{\frac{x}{\sqrt{2\Delta}}} + 2 \int_{\frac{x}{\sqrt{2\Delta}}\frac{\sigma_y}{\sigma_x}}^{\frac{x}{\sqrt{2\Delta}}} e^{t^2} dt\right\}
$$

$$= -\sqrt{\frac{2\pi}{\Delta}}\frac{x}{\Delta}e^{-\frac{x^2}{2\Delta}}[\mathrm{erfi}(\frac{x}{\sqrt{2\Delta}}) - \mathrm{erfi}(\frac{x}{\sqrt{2\Delta}}\frac{\sigma_y}{\sigma_x})] - \frac{2}{\Delta}[e^{-\frac{x^2}{2\sigma_x^2}}\frac{\sigma_x}{\sigma_y} - 1] \ .$$

Either by a similar integration or by using $i\mathrm{erfi}(-ix) = \mathrm{erf}(x)$ one obtains

$$\partial_x U|_{x=0} = 0 \ , \tag{48}$$

$$\partial_x^2 U|_{x=0} = \frac{2}{\Delta}(\sqrt{\frac{\pi}{2\Delta}}ye^{\frac{y^2}{2\Delta}}[\mathrm{erf}(\frac{y}{\sqrt{2\Delta}}\frac{\sigma_x}{\sigma_y}) - \mathrm{erf}(\frac{y}{\sqrt{2\Delta}})] + e^{-\frac{y^2}{2\sigma_y^2}}\frac{\sigma_y}{\sigma_x} - 1) \ , \tag{49}$$

$$\partial_y U|_{x=0} = -\sqrt{\frac{2\pi}{\Delta}}e^{\frac{y^2}{2\Delta}}[\mathrm{erf}(\frac{y}{\sqrt{2\Delta}}\frac{\sigma_x}{\sigma_y}) - \mathrm{erf}(\frac{y}{\sqrt{2\Delta}})] \ , \tag{50}$$

$$\partial_y^2 U|_{x=0} = -\frac{2}{\Delta}(\sqrt{\frac{\pi}{2\Delta}}ye^{\frac{y^2}{2\Delta}}[\mathrm{erf}(\frac{y}{\sqrt{2\Delta}}\frac{\sigma_x}{\sigma_y}) - \mathrm{erf}(\frac{y}{\sqrt{2\Delta}})] + e^{-\frac{y^2}{2\sigma_y^2}}\frac{\sigma_x}{\sigma_y} - 1) \tag{51}$$

The Laplace equation for the projected electrostatic potential of the proton beam with charge λ per unit length is implicit in these formulas due to

$$(\partial_x^2 + \partial_y^2)\frac{\lambda}{4\pi\varepsilon_0}U(x,y)|_{x=0} = -\frac{\lambda}{4\pi\varepsilon_0}\frac{2}{\sigma_x\sigma_y}e^{-\frac{y^2}{2\sigma_y}} = -\frac{\lambda}{\varepsilon_0}\int_{-\infty}^{\infty}\rho(0,y,z)dz \ . \tag{52}$$

4 Emittance measurements with wire scanners

In HERA six wire scanners (4 in the p-ring and 2 in the e-ring) are installed to measure the beam size ($\sigma_{x,y}$) to determine the beam emittance according to the relation:

$$\epsilon_{x,y} = \frac{\sigma_{x,y}{}^2}{\beta_{x,y}}, \tag{53}$$

where the beta-function $\beta_{x,y}$ at the position is known from the theoretical optic. The relevant parameters of the wire scanners for luminosity optics (e-ring: "helumgj", p-ring: "hpl920e+") are summarized in table 8. For a horizontal wire only the horizontal beta-function and the dispersion are given, while for a vertical wire only the vertical beta-function is given. For the design emittances (see table 1) the corresponding design beam sizes are also included in the table. A photo of the horizontal and vertical wirescanners OL 8 in the HERA e-ring is shown in Fig. 11. The scattered electrons are detected with a photomultiplier and scintilator which is located before the HERMES experiment, a photo is shown in Fig. 12. The p-ring wire scanners WR 123 and WR 85 are used to measure the average beam size of all bunches, while the other wire scanners can can be used to measure the beam size of individual bunches or almost individual bunches (average over 3 bunches).

name	s / m	β_x/m	D_x	β_y/m	σ_x/mm	σ_y/mm
	HERA-p		$\epsilon_{Npx} = 20\ \mu$m, $\epsilon_{Npy} = 20\ \mu$m			
WR 123	123.59 WR	238.4	-0.077		1.102	
WR 85	84.97 WR			151.0		0.877
WR 19	19.91 WR	38.6	-0.593		0.444	
WR 22	20.57 WR			39.9		0.446
	HERA-e		$\epsilon_{ex} = 20.0$ nm, $\epsilon_{ey} = 3.4$ nm			
OL 8 h	8.02 OL	25.1	-0.029		0.708	
OL 8 v	8.17 OL			36.6		0.353

Table 8: Wire scanners in the HERA-p and HERA-e ring.

The precision of the emittance measurements depends on the precision with which the beam width can be measured *and* on the error of the beta-function:

$$\frac{\Delta\epsilon}{\epsilon} \approx -\frac{\Delta\beta}{\beta} + 2\frac{\Delta\sigma}{\sigma}. \tag{54}$$

The typical error for the beta-functions in a large machine like HERA is about 15 %. Some measurements of the beta-functions during the commissioning phase of HERA indicate even larger errors of up to 50 %. The error in the measured beam size $\Delta\sigma$ depends on the wire. Some signals from the e-ring wire scanners OL 8 were very noisy during the measurements in June 2002. The results from

the p-ring wire scanners seem to be more reliable. From this it follows that the error in the emittance measurement is therefore at least 20 %. Some results from measurements in June 2002 are discussed in the next subsection.
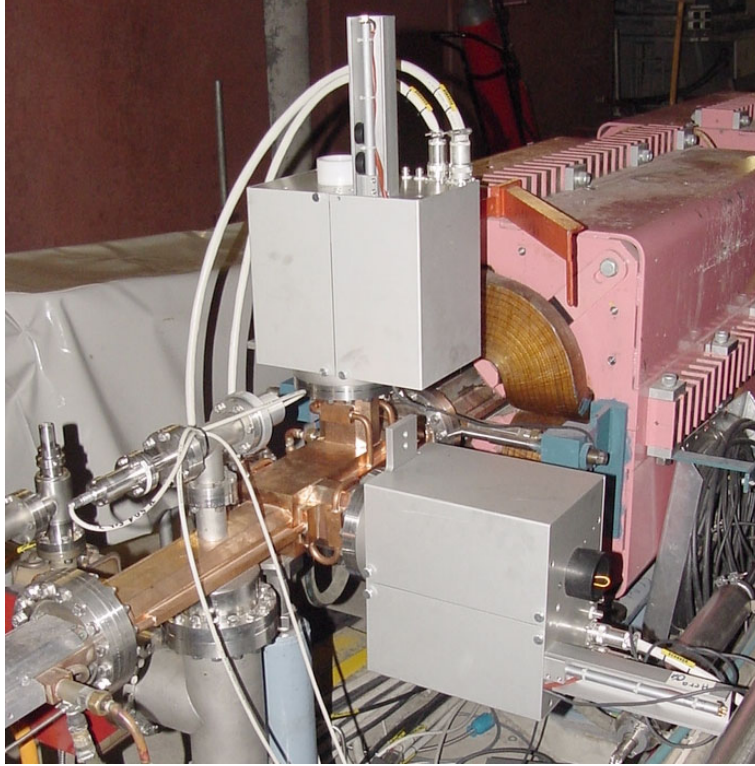

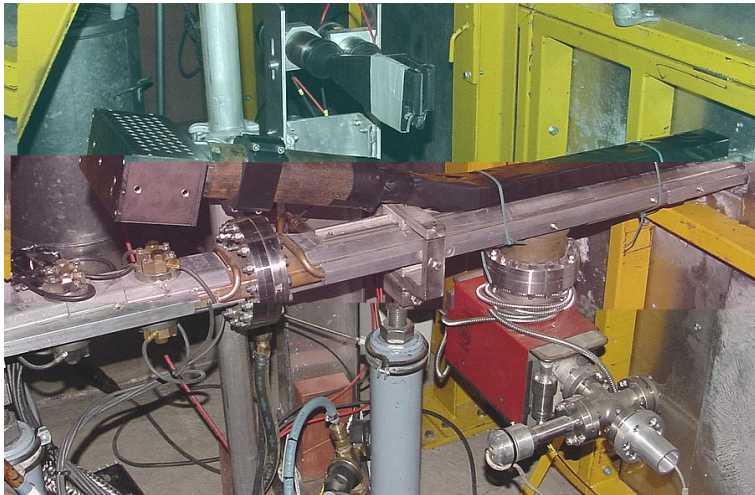Figure 11: HERA tunnel: the wire scanners in the e-ring.

Figure 12: HERA tunnel: the photomultiplier and the scintilator in the e-ring are used to detect the scattered electrons from the wire scanner OL 8.

... ularly to determine the
... m. As an example we
... n horizontal wire scans
... positron bunch in one
... ge from several bunches
... from one single bunch
... recently improved, see
... uld only be determined
... ne sigma beam size of
... ign value of 0.709 mm.
... urves which correspond
... at the accuracy of these

data

59   60   61   62
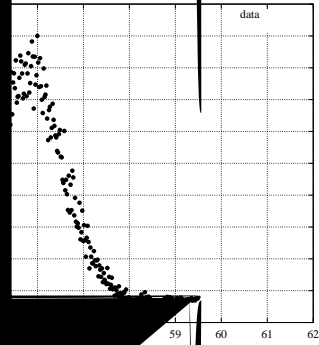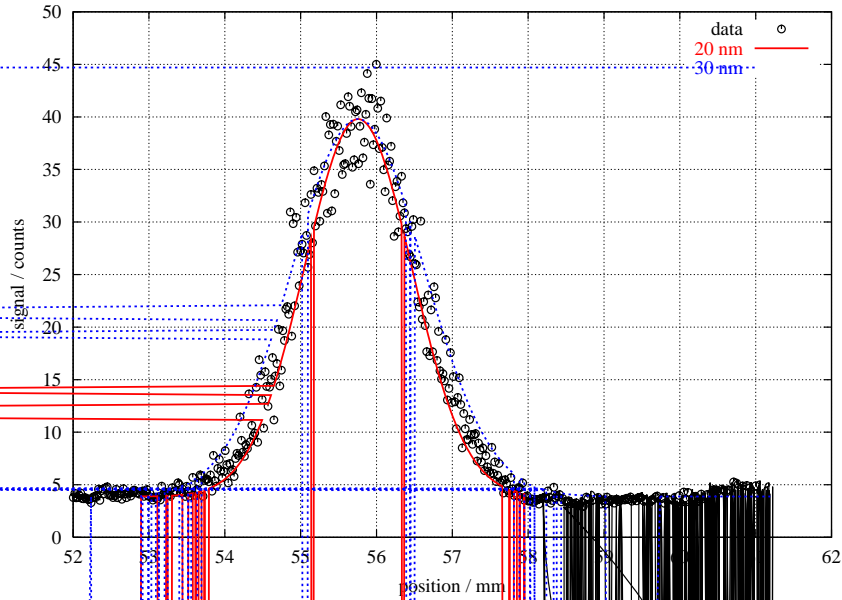
Figure 14: Averaged signal from several horizontal wire scans with the e-ring wire OL 8. The curves correspond to an emittance of 20 nm or 30 nm or a beam size of 0.709 mm and 0.868 mm.
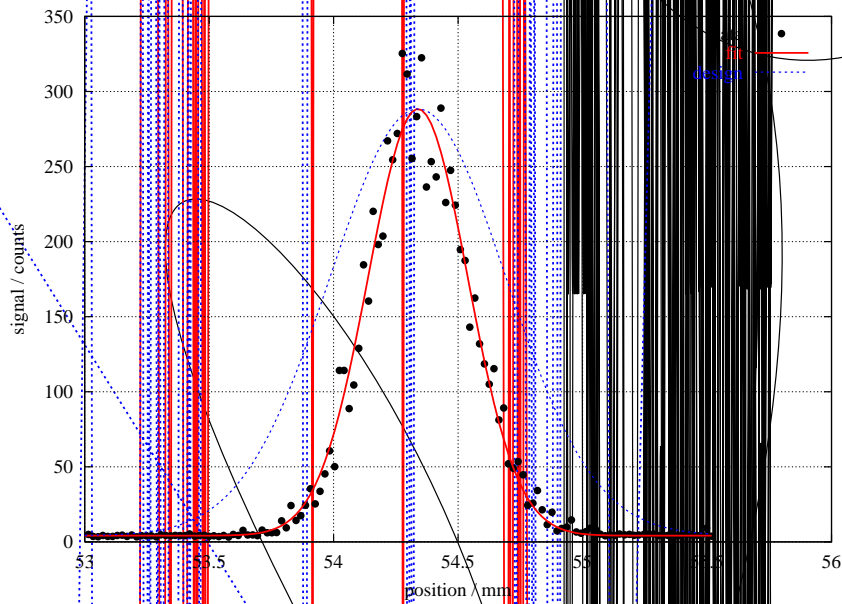
Figure 15: Vertical wire scan with the e-ring wire OL 8, averaged signal from 14 bunches. The fit gives a beam size of $\sigma_y = 0.1998$ mm. The design beam size is $\sigma_y = 0.353$ mm which is presented by a dashed curve.

5 Measurements in June 2002

In June 2002 the effective beam size of the colliding proton and positron beams have been measured using a luminosity scan, which means that the specific luminosity was measured versus the amplitude of the bump used to separate the beams. The theory of the measurement has been discussed in section 3 of this report.

After these measurements in June it has been found that the luminosity optic magnet file was not properly configured in the HERA interaction region. The beta-functions were larger than the design values (see table 3) due to a corrupted file with wrong set-points for the magnet currents. Nevertheless we will shortly report on these measurements since even for this perturbed optics one can use luminosity scans to crosscalibrate beam size measurements and luminosity measurements.

5.1 Luminosity scan at H1

The luminosity scan at H1 was performed on June 10, 2002 after 5 a.m. using the third positron refill on the same proton fill. During the measurement 10 proton bunches with a total current of about 3 mA and 12 positron bunches with a total current of about 2.5 mA were stored in HERA. The horizontal and vertical beam profiles of the proton beam have been measured with the WR 19 and WR 22 wire scanners. Fits to the data are shown in Fig. 16. The measured beam

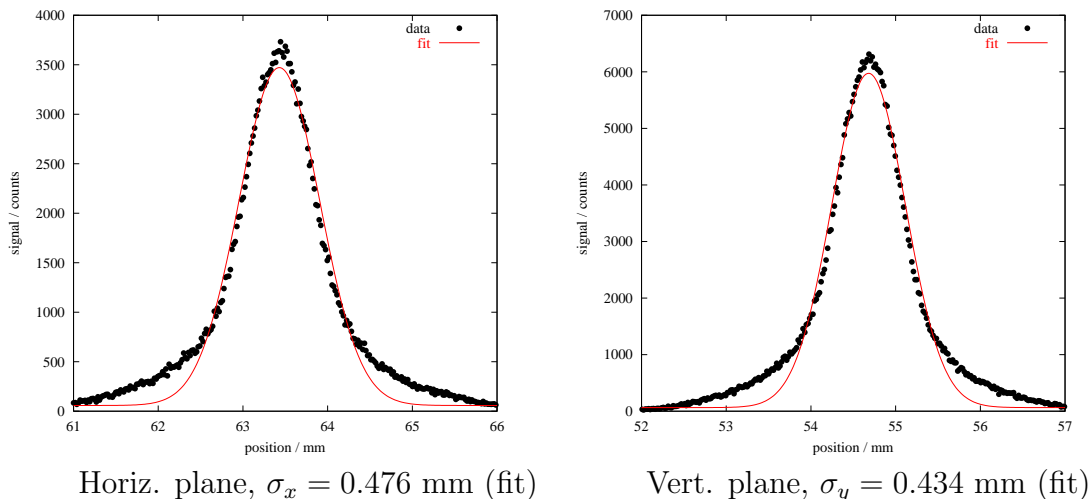Horiz. plane, $\sigma_x = 0.476$ mm (fit)   Vert. plane, $\sigma_y = 0.434$ mm (fit)

Figure 16: Wire scans in the horizontal and vertical plane to measure the beam width of the proton beam (average over 3 bunches).

width (one sigma) is 0.476 mm in the horizontal and 0.434 mm in the vertical plane, corresponding to an invariant (two sigma) emittance of 23 mm mrad in the horizontal and 18.5 mm mrad in the vertical plane assuming the beta-functions

from table 8. The proton beam had developed clearly visible tails at the time of the measurements.

Using the wire scanners OL 8 h and OL 8 v the horizontal and vertical profile of the positron has been measured. The results of the measurements and a fit to the data are shown in Fig. 17. The poor fit to the horizontal data gives a beam width (one sigma) of 0.766 mm which corresponds to an emittance of about 20 nm assuming the beta-function from table 8. The vertical fit gives a (one sigma) beam width of 0.226 mm which corresponds to an emittance of about 1.4 nm in the vertical plane. The vertical emittance is therefore smaller than the design value (see table 1) of 3.4 nm. The beam emittance has been calculated from the theoretical optic. The error of the beta-function may be large since the optic was perturbed in the interaction region.

60 –   –

40 –   –

20 –   –

0 –   –

luminosity of only $0.97 \cdot 10^{30} \ \text{sec}^{-1} \ \text{cm}^{-2} \ \text{mA}^{-2}$ during the measurements, which is only 83 % of the expected specific luminosity.

The measured photon (rms) spot size at the lumi detector was 15.87 mm in the horizontal plane and 10.05 mm in the vertical plane. These numbers differ from the theoretical values and support the finding that the correct optic was not set during the run. The first positron bunch was colliding with a proton bunch with an intensity of 139 μA. The measured beam-beam tune shift was 0.084 kHz for the horizontal tune and 0.133 kHz for the vertical tune.
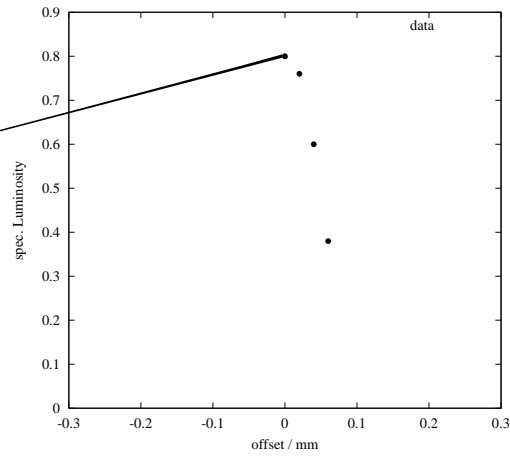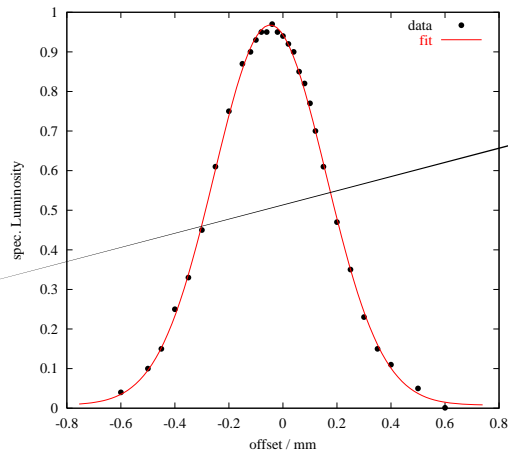
Horiz. plane, $\sigma_{eff,x} = 146.5 \ \mu$m

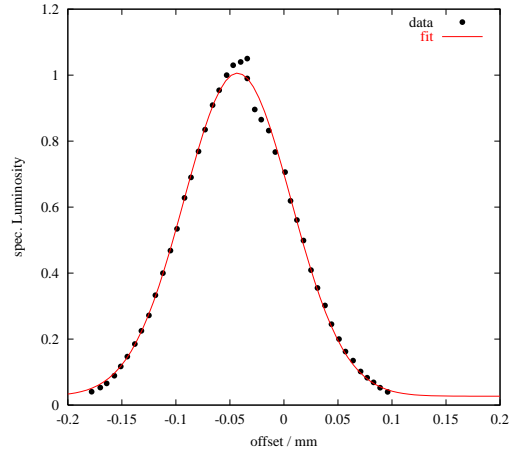in the horizontal and the vertical plane. The expected specific luminosity is:

$$\mathcal{L}_{s\,0} = \frac{1}{e^2\,f_0}\,\frac{0.922}{4\pi\,144.3\,\mu\mathrm{m}\,35.1\,\mu\mathrm{m}} = 1.19 \cdot 10^{30}\ \mathrm{sec}^{-1}\ \mathrm{cm}^{-2}\ \mathrm{mA}^{-2}. \qquad (58)$$

The hourglass effect (factor 0.922) is included for a proton bunch length of 1.4 ns (FWHM) obtained from the HERA archive. During the luminosity scan the maximum measured value for the specific luminosity was $1.05\cdot10^{30}$ sec^{-1} cm^{-2} mA^{-2}, which is 88 % of the expected value.

The size of the photon beam spot at the ZEUS luminosity monitor was not documented in the HERA logbook, and the beam-beam tune shift was not measured.
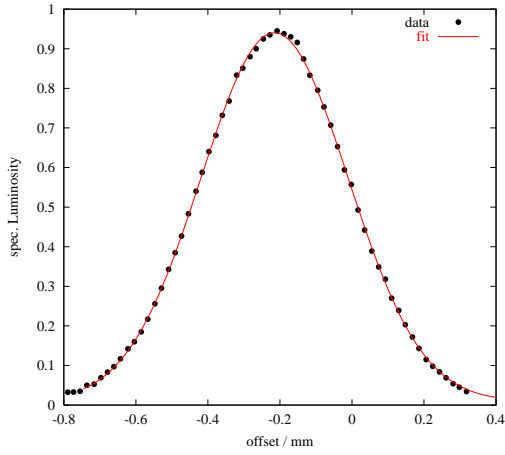

Horiz. plane,$\sigma_{eff,x} = 144.3\ \mu$m   Vert. plane,$\sigma_{eff,x} = 35.1\ \mu$m

Figure 19: Specific luminosity versus horz. and vert. bump amplitude at the ZEUS experiment.

6 Measurements from October 2002

The luminosity scans at the H1 and ZEUS experiments have been repeated on October 1, 2002 (night-shift Sep. 30/Oct 1). Before these measurements were done the optics problems in the positron ring had been fixed due to the efforts of the task forces on optics. We shortly report on these recent results starting with results from the emittance measurements of the positron beam. The horizontal and vertical beam profile of the first positron bunch is shown in Fig. 20 as measured on Oct. 1. The signal quality is much better compared to beam profiles measured in June (see Fig. 13) since the position of the photomultiplier has been optimized. The measured beam width corresponds to an emittance (one sigma)
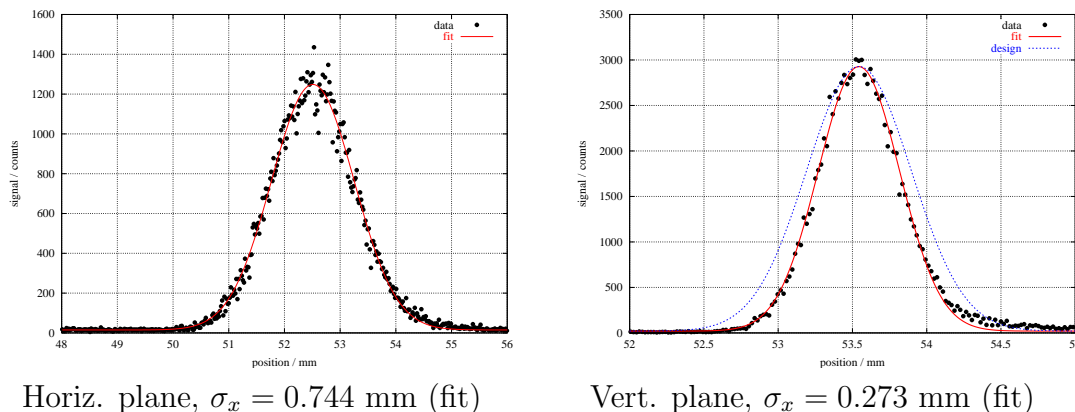
Horiz. plane, $\sigma_x = 0.744$ mm (fit)   Vert. plane, $\sigma_x = 0.273$ mm (fit)

Figure 20: Wire scans in the horizontal and vertical plane to measure the beam width of the positron beam.

of $\epsilon_{ex} = 22$ nm and $\epsilon_{ex} = 2$ nm assuming the beta-functions from table 8. For the proton beam an invariant emittance (two sigma) of about $\epsilon_{Npx} = 15$ mm mrad and $\epsilon_{Npy} = 16$ mm mrad has been calculated from wire scan measurements with the wire scanners WR 19 and WR 22. Using the design beta-functions at the interaction point from table 1 one obtains for the measured emittances the following effective beam sizes and specific luminosity:

$$\sigma_{eff,x} = 107.3 \ \mu\text{m}, \quad \sigma_{eff,y} = 25.8 \ \mu\text{m}, \quad \mathcal{L}_s = 2.1 \cdot 10^{30} \, \text{s}^{-1} \, \text{cm}^{-2} \, \text{mA}^{-2}. \quad (59)$$

A reduction due the hourglass effect by a factor of 0.899 has been taken into account based on a measured length of the proton bunch of 1.7 ns (FWHM). During the measurements a total proton current of 11.9 mA was stored in 60 bunches and a total positron current of 2.9 mA in was stored 63 bunches. 39 bunches were colliding. The single bunch intensities for the protons was only 40 % and for the positrons only 24 % of the assumed values in table 1, which are already smaller than the design values.

6.1 Luminosity scan at H1

The luminosity scan at H1 was performed on Oct 1, 2002 after 1:00 a.m.. The specific luminosity as function of the bump amplitude is shown in Fig. 21. A simple fit gives an effective beam size at the interaction point and a (calculated) specific luminosity of:

$$\sigma_{eff,x} = 109.8 \ \mu m, \quad \sigma_{eff,y} = 24.3 \ \mu m, \quad \mathcal{L}_s = 2.2 \cdot 10^{30} \, \mathrm{s}^{-1} \, \mathrm{cm}^{-2} \, \mathrm{mA}^{-2}. \quad (60)$$

(The hourglass effect is included as a factor of 0.899). These data are in good agreement with the prediction from the measured emittances and the theoretical beta-function (see Eqn. 59). The maximum specific luminosity of $1.82 \cdot 10^{30} \, \mathrm{s}^{-1} \, \mathrm{cm}^{-2} \, \mathrm{mA}^{-2}$ was measured during the horizontal scan, which is only 83 % of the expected value. The specific luminosity was even lower during the vertical scan which indicates that there was a horizontal offset during that measurement.
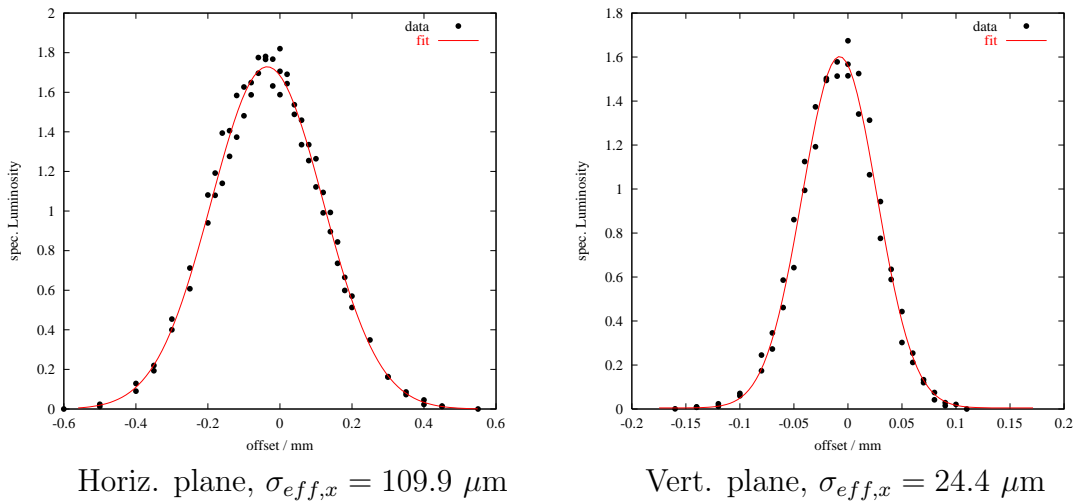

Horiz. plane, $\sigma_{eff,x} = 109.9 \ \mu m$ Vert. plane, $\sigma_{eff,x} = 24.4 \ \mu m$

Figure 21: Specific luminosity versus horz. and vert. bump amplitude at the H1 experiment.

6.2 Luminosity scan at ZEUS

The corresponding luminosity scan at ZEUS was performed during the same run on Oct 1, 2002 after 3:00 a.m.. The results are shown in Fig. 22. A simple fit gives an effective beam size at the interaction point and a (calculated) specific luminosity of:
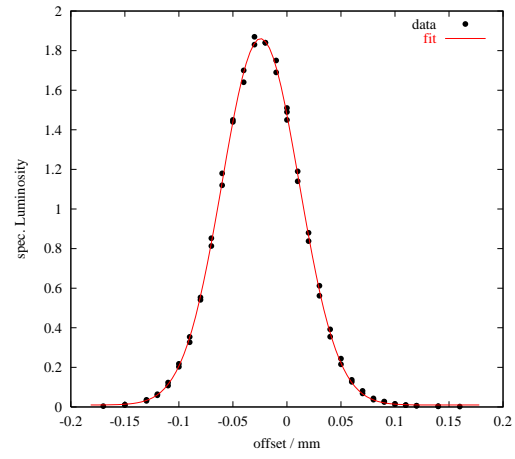
$$\sigma_{eff,x} = 115.6 \ \mu m, \quad \sigma_{eff,y} = 25.2 \ \mu m, \quad \mathcal{L}_s = 2.0 \cdot 10^{30} \, \mathrm{s}^{-1} \, \mathrm{cm}^{-2} \, \mathrm{mA}^{-2}. \quad (61)$$

(The hourglass effect is included as a factor of 0.899), which is again in good agreement with the predictions (Eqn. 59). The maximum specific luminosity of

$1.87 \cdot 10^{30}\,\mathrm{s}^{-1}\,\mathrm{cm}^{-2}\,\mathrm{mA}^{-2}$ was measured during the vertical scan, which is 93 % of the expected value. The specific luminosity was lower during the horizontal scan which indicates that there was a vertical offset during that measurement.
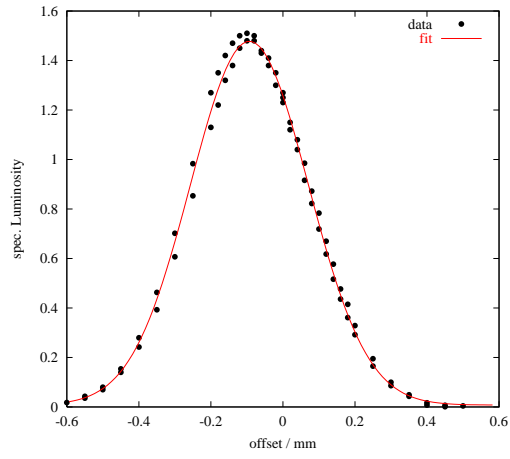
Horiz. plane, $\sigma_{eff,x} = 115.6\ \mu$m   Vert. plane, $\sigma_{eff,x} = 25.2\ \mu$m

Figure 22: Specific luminosity versus horz. and vert. bump amplitude at the ZEUS experiment.

7 Conclusions

This report summarizes the measurements of the effective beam size at the interaction point using luminosity scans from June and October 2002 and the theory needed to evaluate the measurements.

The parameters and the optic of the upgrade HERA interaction region were introduced in detail and several effects which may cause a degradation of the luminosity were discussed. The hourglass effect, dominated by the proton bunch length, reduces the luminosity typically by about 10 %. It was found that the dynamic beta-function for the positrons at the interaction point can be up-to 35 % larger than the nominal ones depending on proton intensity and the betatron-tune of the positrons and therefore the beam–beam kick has to be taken into account when the optics is computed.

An important diagnostic tool are the wire scanners in the HERA e- and p-ring. The results obtained after the commissioning of the wire scanners were discussed in a separate section. The signal quality for a single positron bunch was initially rather poor, but the performance of wire scanner OL 8 was greatly improved due to efforts of the diagnostic group MDI. The positron wire scanner can only be used up-to a total positron current of 6 mA which was fulfilled during the machine studies. The design emittance ratio $\epsilon_{ey}/\epsilon_{ex} = 0.17$ is rather large. During the luminosity scans a ratio of 0.07 (June) and 0.09 (Oct.) was measured assuming the theoretical beta-function at the position of the wire scanner. Optic measurements indicate that the error in the beta-function in October was not larger than 15 %.

The design single bunch currents are $307\,\mu A$ for the positron beam and $778\,\mu A$ for the proton beam (corresponding to total currents of $I_e = 58$ mA and $I_e = 140$ mA). All lumiscans were performed at much lower single bunch intensities:

measurement	e^+	p
June 10 (H1)	208 μA	300 μA
June 25 (ZEUS)	150 μA	200 μA
Oct 1 (H1, ZEUS)	46 μA	198 μA

The measurements in June clearly indicat that the beam size at the interaction point was larger by a factor of up-to 1.7 than that calculated from the measured emittances and the theoretical beta-functions. Furthermore the luminosity measured with the luminosity monitor of the experiments was about 15 % lower than that expected from the measured effective beam size at the interaction point. The problems with the luminosity optic magnet file were later confirmed and fixed by the task forces on optics.

All known optics problems were fixed before the luminosity scan on Oct. 1, 2002. The agreement between the calculated beam sizes based on the measured emittances and theoretical beta-function and the measurements are very good for both interaction regions:

measurement	σ_x/mm	σ_y/mm
calculated	107.3	25.8
H1	109.8	24.3
ZEUS	115.6	25.2.

The maximum measured luminosity during the the luminosity scan was $1.82 \cdot 10^{30}\,\mathrm{s}^{-1}\,\mathrm{cm}^{-2}\,\mathrm{mA}^{-2}$ at H1 and $1.87 \cdot 10^{30}\,\mathrm{s}^{-1}\,\mathrm{cm}^{-2}\,\mathrm{mA}^{-2}$ at ZEUS, which is 83 % (H1) and 93 % (ZEUS) of the expected value. The differences could be due to errors in the emittance measurements, calibration errors of the luminosity monitors, a crossing angle or local coupling at the interaction point. There are no indications of any severe problems with respect to the measured specific luminosities for low proton and positron intensities.

But for higher proton intensity the specific luminosity seems to be lower. Data from the HERA archive are shown in Fig. 23 for a time period of 8 days from Sep. 26 to Oct. 3, 2002. The single bunch current of the 5th proton and
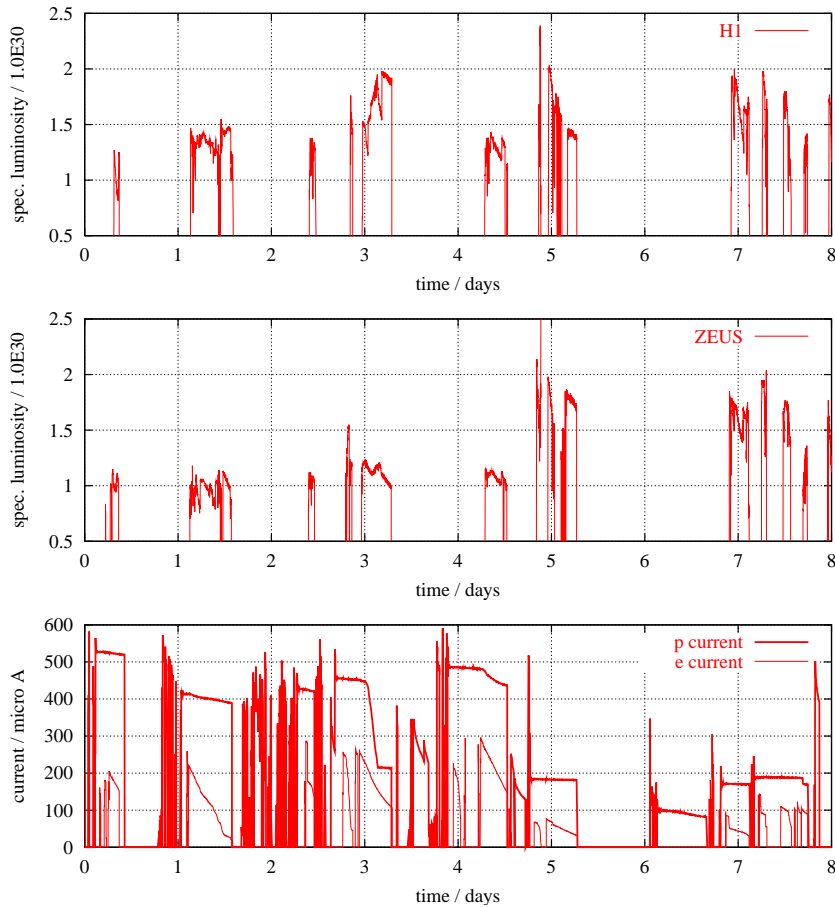

Figure 23: Data from the HERA archive from Sep. 26, 2002 to Oct. 3, 2002.

positron bunches are shown in the graph at the bottom (the thick line is the

34

proton current). The specific luminosity at H1 is shown in the top graph, while the corresponding ZEUS data are shown in the graph in the middle of Fig. 23. In the figure day "5" is Oct. 1, 2002 when the luminosity scan was done using a single bunch proton current of about 200 μA. In the runs before Oct. 1 proton single bunch currents between 400 μA and 520 μA were used. During these runs the specific luminosity was always below $1.5 \cdot 10^{30} \, \mathrm{s}^{-1} \, \mathrm{cm}^{-2} \, \mathrm{mA}^{-2}$. This may indicate that beam-beam effects affect the specific luminosity for proton single bunch intensities above 200 μA (or total currents of more than 36 mA).

The luminosity scans were done with betatron tunes of the positron beam close to the working point $Q_{ex} = 54.239$ and $Q_{ex} = 51.315$. This working point was predominantly used for nearly all luminosity runs in the year 2002. A few attempts have been made at the end of October to collide beams with tunes close to $Q_{ex} = 54.102$ and $Q_{ex} = 51.213$, which have been used to get good polarization in the year 2000. It was difficult to run with a tune close to $Q_{ex} = 54.102$ and $Q_{ex} = 51.213$ due to nonlinear resonances and synchrotron- betatron resonances. This indicates the difficulty in finding a working point for the positron beam which is simultaneously good for positron proton collision and high polarization.

Acknowledgment

References

[1] G. Hoffstaetter, *Future Possibilities for HERA* EPAC 2000, Vienna, June 2000

[2] M. Bieler et al., *Experiments about the Beam-Beam Effect at HERA*, in HERA Acc. Studies 1999, ed. G.H. Hoffstaetter, DESY HERA 00-02, May 2000

[3] B. Holzer, plot of the lattice configuration in the HERA interaction regions.

[4] E. Gianfelice, computer code to calculate and plot the HERA bumps.

[5] H. Grote, F.C. Iselin, *The MAD Program, Version 8.19* CERN/SL/90-13 (AP) (Rev.5)

[6] M. Sands, *The Physics of Electron Storage Rings*, SLAC-121 (1970)

[7] PETROS Program
J. Kewisch *Berechnung der linearen, gekoppelten Optik und der Strahlparameter im Elektronenringbeschleunigern unter Berücksichtigung von Magnetfeldern*, Diploma Thesis

[8] R. Brinkmann, *Determination of HERA Specific Luminosity from Beam Separation Scans*, DESY HERA, Technical Note 94-03, Aug 1994

[9] E. Keil, *Beam-Beam Dynamics*, CERN SL/94-78 (AP),1994

[10] *HERA Acc. Studies 2000*, ed. G.H. Hoffstaetter, DESY HERA 00-07, November 2000

[11] G.H. Hoffstaetter, *Luminosity scans for a 60° and a 72° optics in HERA-e* in [10], *Optimized luminosity scans for a spinmatched 72∘ optics in HERA-e* in [10], *Luminosity scans in HERA* in Proceedings of EPAC'02, June 2002

[12] S. van der Meer, *CERN–ISR–PO/68–31* (1968)

[13] D. P. Barber, The generalization of the van der Meer method to include the case of bunched collinear beams, *Daresbury Nuclear Physics Laboratory, CERN Preprint* (1973)

[14] E. Keil, Beam–Beam Dynamics, *CERN SL/94–78 (AP)* (1994)